Electronic Supplementary Information† (ESI†)

Fluorimetric sensing of Pb^{2+} and CrO_4^{2-} ions through host-guest inclusion for human lung cancer live cell imaging †

S. Mohandoss[a], J. Sivakamavalli[b], B. Vaseeharan[b] and T. Stalin[a]*

[a]*Department of Industrial Chemistry, School of Chemical Sciences, Alagappa University, Karaikudi- 630 003, Tamilnadu, India.*

[b]*Department of Animal Health and Management, Alagappa University, Karaikudi- 630 003, Tamilnadu, India.*

**Corresponding author (Dr. T. Stalin)*

E-mail: tstalinphd@rediffmail.com, drstalin76@gmail.com; Mobile: +91 9944266475

Contents

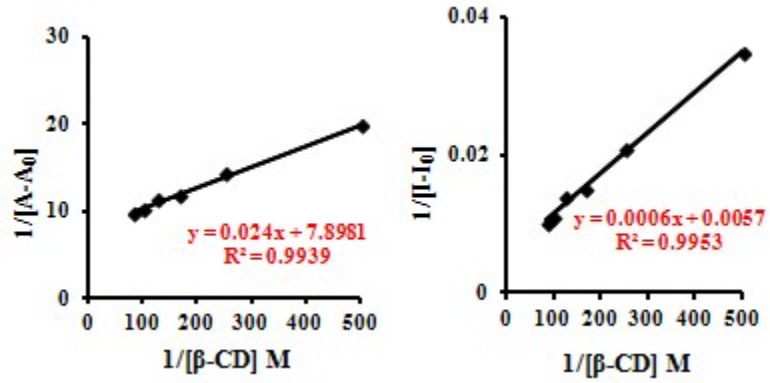

Figure S1: Benesi–Hildebrand plot of probe **2** (a) $1/[A-A_0]$ vs. 1/[β-CD] and (b) $1/[I-I_0]$ vs. 1/[β-CD].

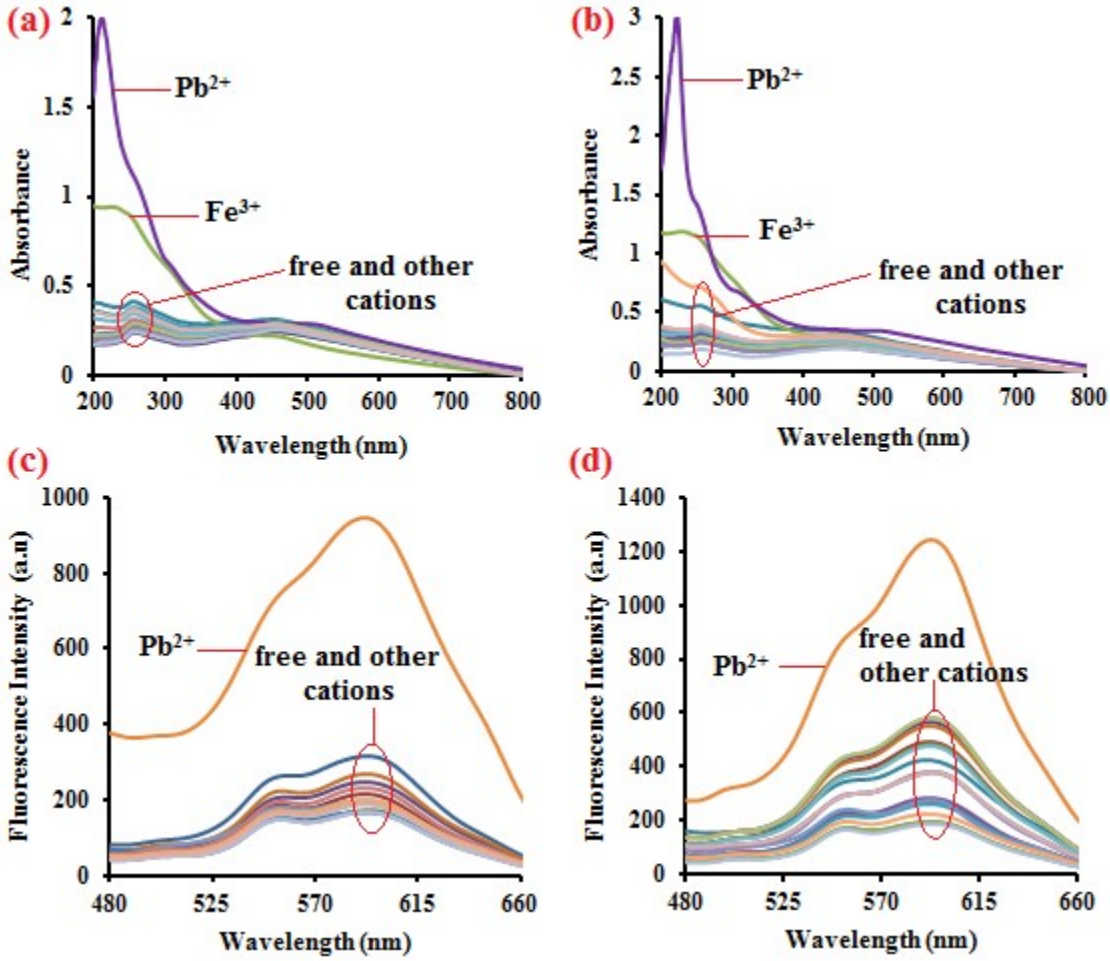

Figure S2: Absorption spectra of (a) **1** (b) **2** and fluorescence spectra of (c) **1** (d) **2** (**1**;1 x10^{-4} M, β-CD;1.2x10^{-2} M) in pH~7.5 solution in presence of different cations (1x10^{-4} M).

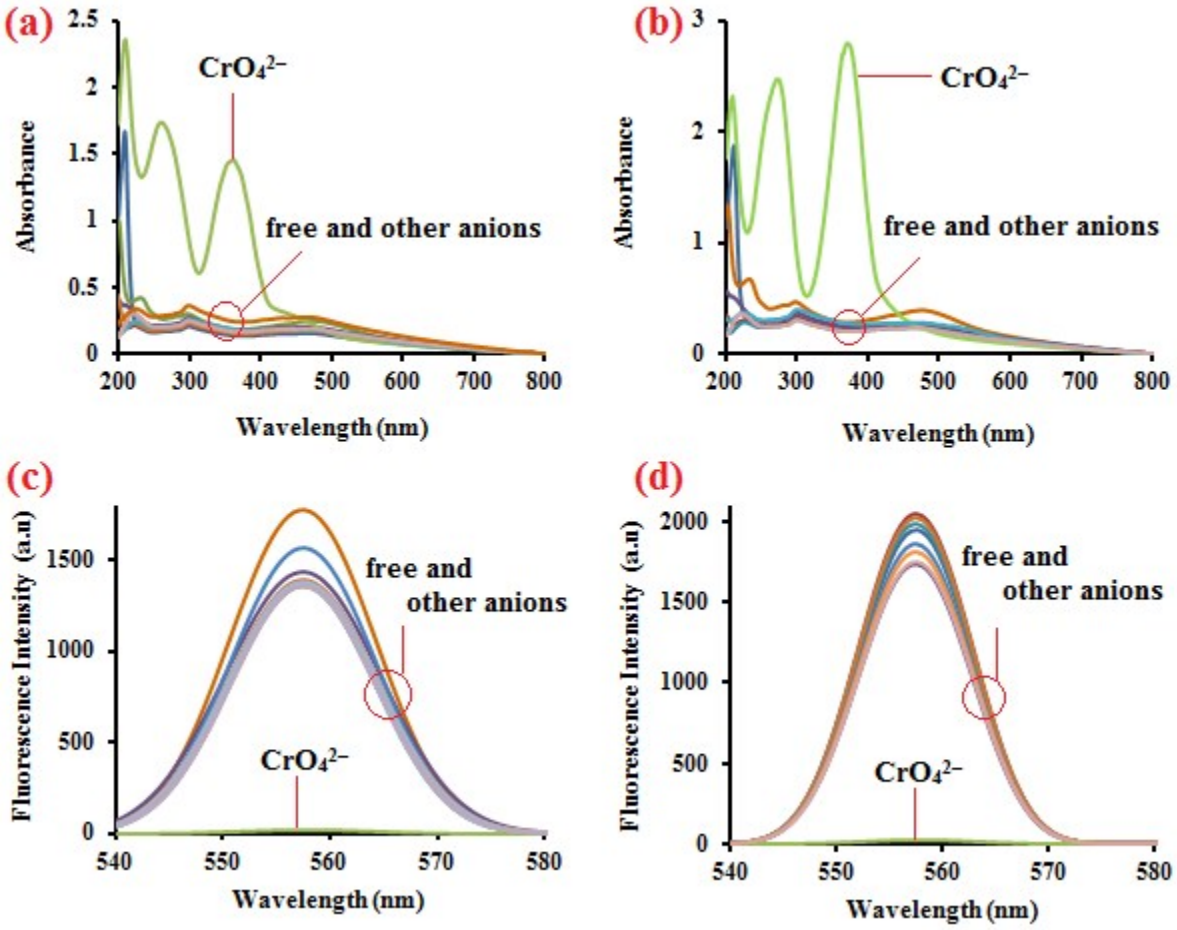

Figure S3: Absorption spectra of (a) **1** (b) **2** and fluorescence spectra of (c) **1** (d) **2** (**1**;1x10^{-4} M, β-CD;1.2x10^{-2} M) in pH~7.5 solution in presence of different anions (1x10^{-4} M).

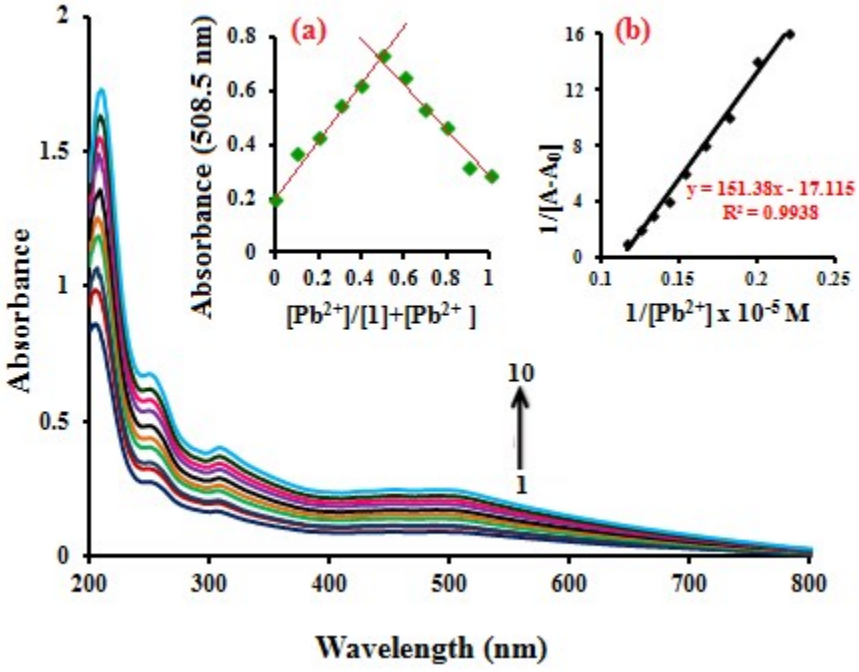

Figure S4: Absorption spectra of **1** (**1**;1x10^{-4} M) with the addition of Pb^{2+} ion concentrations (4.0x10^{-5} – 8.5x10^{-5} M). Inset figures (a) Job's plot analysis for the complexation between **1** and Pb^{2+} ion and (b) Benesi–Hildebrand plot of $1/[A-A_0]$ vs. $1/[Pb^{2+}]$.

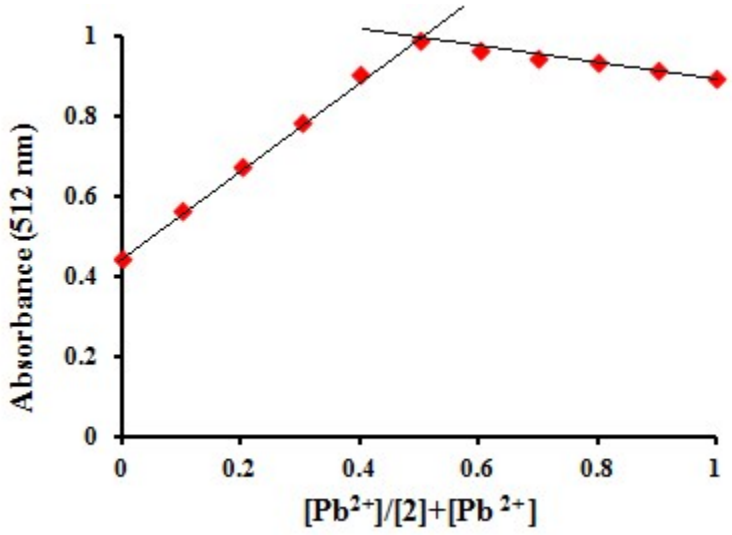

Figure S5: Job's plot analysis for the complexation between **2** and Pb^{2+} ion.

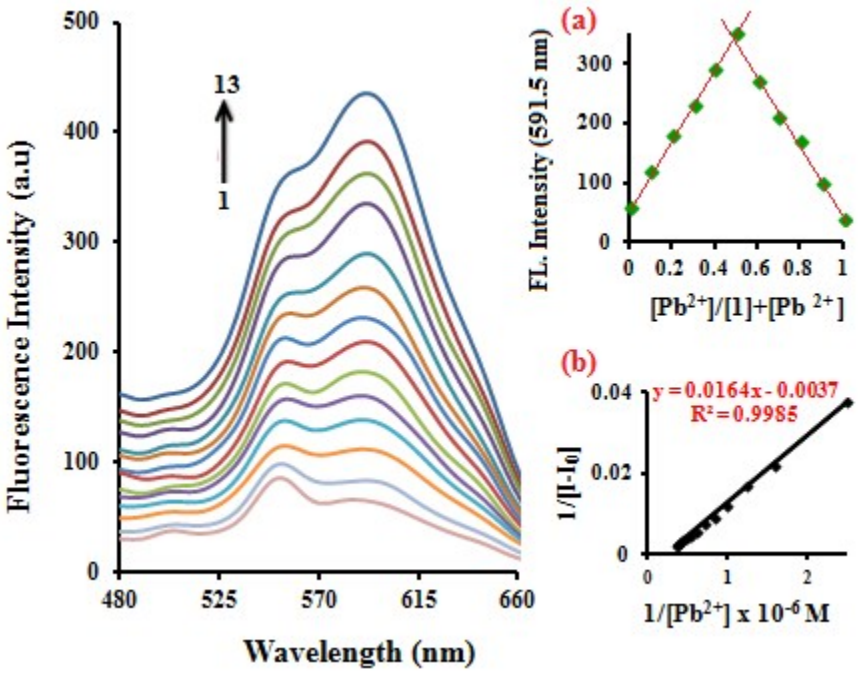

Figure S6: Fluorescence spectra of **1** (**1**;1x10^{-4} M) with the addition of Pb^{2+} ion concentrations (0.2x10^{-6} – 2.8x10^{-6} M). Inset figures (a) Job's plot analysis for the complexation between **1** and Pb^{2+} ion and (b) Benesi–Hildebrand plot of $1/[I-I_0]$ vs. $1/[Pb^{2+}]$.

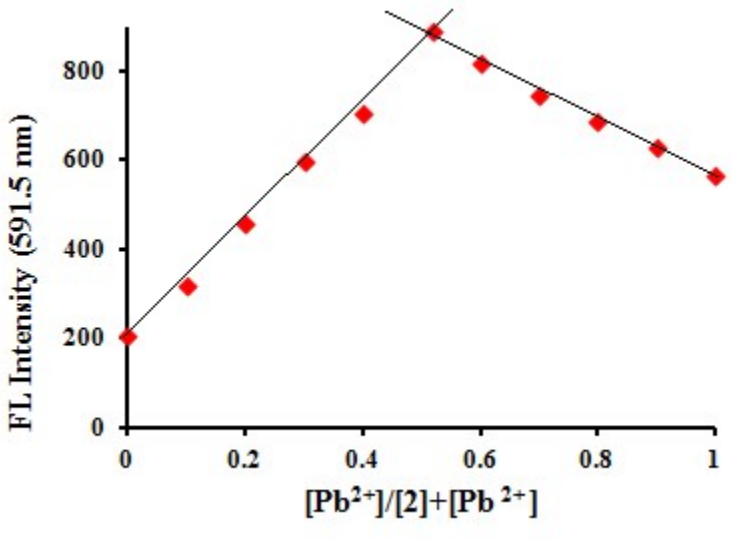

Figure S7: Job's plot analysis for the complexation between **2** and Pb^{2+} ion.

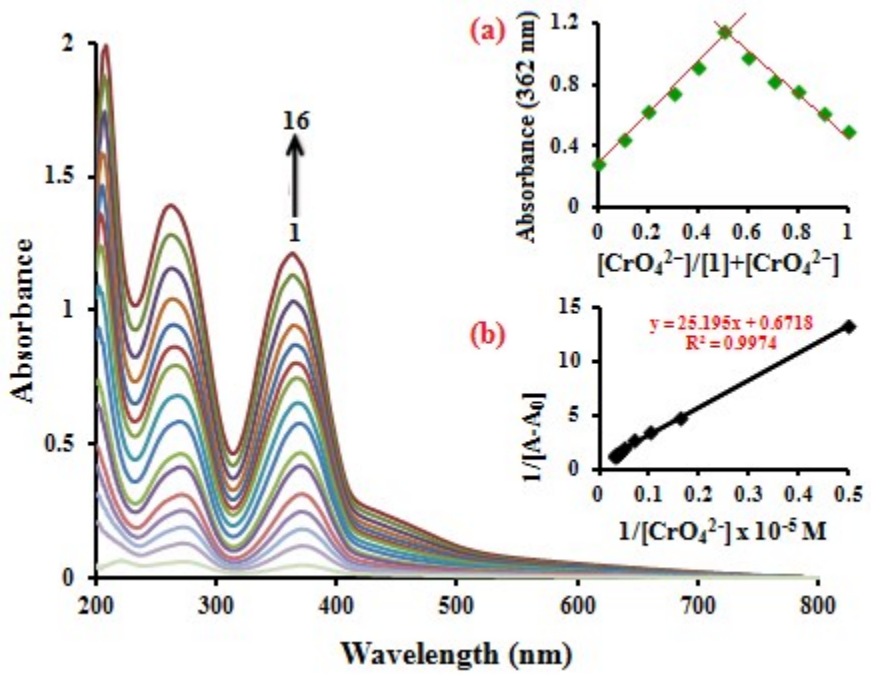

Figure S8. Absorption spectra of **1** (**1**;1x10^{-4} M) with the addition of CrO_4^{2-} ion concentrations (2x10^{-5} – 32x10^{-5} M). Inset figures (a) Job's plot analysis for the complexation between **1** and CrO_4^{2-} ion and (b) Benesi–Hildebrand plot of $1/[A-A_0]$ vs. $1/[CrO_4^{2-}]$.

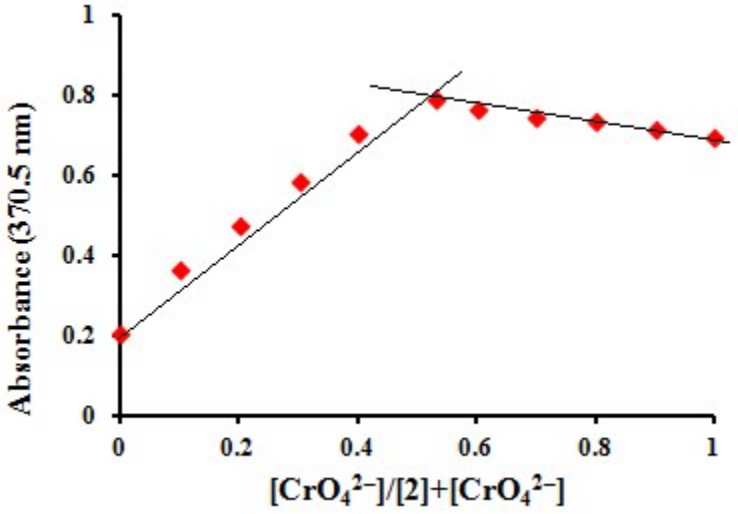

Figure S9: Job's plot analysis for the complexation between **2** and CrO_4^{2-} ion.

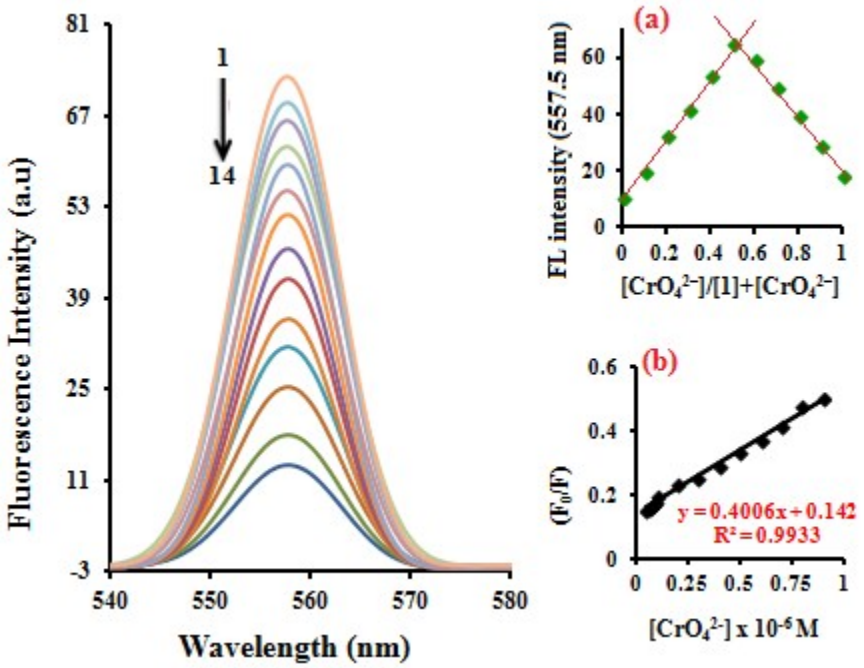

Figure S10: Fluorescence spectra of **1** (**1**;1x10^{-4} M) with the addition of CrO_4^{2-} ion concentrations (0.5x10^{-7} – 0.9x10^{-6} M). Inset figures (a) Job's plot analysis for the complexation between **1** and CrO_4^{2-} ion and (b) Stern-Volmer plot of (F_0/F) vs [CrO_4^{2-}].

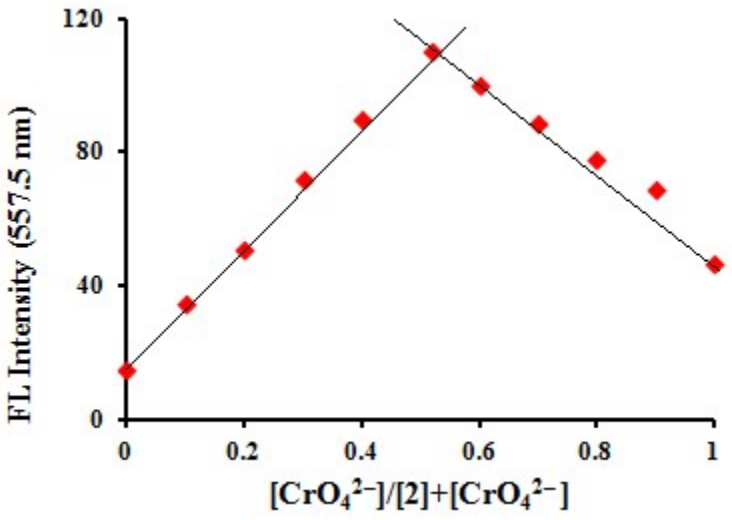

Figure S11: Job's plot analysis for the complexation between **2** and CrO_4^{2-} ion.

Table S1. Absorption and fluorescence maxima (nm) and log ε of **1** at different concentrations of β-CD in pH~7.5 solution.

S.No	Concentration of β-CD (M)	pH~7.5		
		λ_{abs} (nm)	log ε	λ_{flu} (nm)
1	0	480.0	3.79	591.0
	(Without β-CD)	298.5	3.91	
		223.5	3.84	
2	0.002	480.5	3.83	591.5
		298.0	3.95	
		222.5	3.90	
3	0.004	480.5	3.84	591.5
		298.0	3.95	
		222.5	3.91	
4	0.006	480.5	3.84	591.5
		298.0	3.96	
		222.5	3.92	
5	0.008	480.5	3.85	591.5
		298.0	3.98	
		222.0	3.93	
6	0.010	480.5	3.86	591.5
		298.0	3.99	
		222.0	3.97	
		480.5	3.87	591.5
7	0.012	298.0	3.99	
		222.0	4.00	
Binding constant (M^{-1})		361.27		892.88
ΔG (kJ mol^{-1})		-14.83		-17.11

Table S2. Computed using (i) PatchDock and (ii) FireDock server scores of the top 3 docked models of (A) **1**•Pb^{2+}, (B) **1**•CrO_4^{2-} (C) **2**, (D) **2**•Pb^{2+} and (E) **2**•CrO_4^{2-} complex.

(i) Patchdock server					(ii) FireDock server			
Model	S.No.	Score[a]	Area[b] ($Å^2$)	ACE_1[c] kcal/mol	Global Energy[d] kcal/mol	Attractive VdW[e] kcal/mol	Repulsive VdW[e] kcal/mol	ACE_2[f] kcal/mol
A	1	278	33.30	-9.56	4.63	-0.99	0.00	-0.54
	2	266	29.50	-9.56	5.05	-1.27	0.09	0.74
	3	202	25.50	12.91	5.10	-0.93	0.00	-0.54
B	1	1142	131.60	-25.64	-3.80	-3.58	0.02	-1.43
	2	1126	122.70	-23.80	0.70	-2.64	0.00	-1.24
	3	1002	112.50	-23.08	0.83	-3.00	0.00	-1.33
C	1	3048	363.30	-262.60	-43.30	-16.23	2.74	-13.22
	2	3038	374.50	-268.39	-42.89	-16.11	2.78	-13.12
	3	2992	365.20	-271.65	-41.84	-17.11	5.07	-13.12
D	1	3158	384.50	-245.55	-41.62	-18.86	6.40	-11.70
	2	3040	383.40	-243.83	-41.17	-16.87	2.61	-11.67
	3	2994	364.40	-244.30	-40.98	-17.41	3.76	-11.97
E	1	3554	440.90	-310.96	-46.86	-19.33	7.82	-15.22
	2	3438	434.70	-311.90	-45.02	-18.17	4.67	-13.70
	3	3410	441.30	-319.51	-44.59	-19.13	11.11	-15.52

[a]Geometric shape complementarity score

[b]Approximate interface area size of the complex

[c]Atomic contact energy (ACE_1)

[d]Indicating binding energy of the solution.

[e]Representing contribution of the van der Waals forces to the global binding energy.

[f]ACE_2 shows contribution of the atomic contact energy to the global binding energy.